Directional spatial frequency distribution of two dimensional signals

D.E. Hollinberger[1] and P.G. Madhavan[2]

[1] Naval Air Warfare Center, Indianapolis
[2] Electrical Engineering & Computer Science Department
University of Michigan, Ann Arbor
1310 Beal Avenue, Ann Arbor, MI 48109
email: pgmadhav@eecs.umich.edu

ABSTRACT

The time-frequency analysis techniques developed for one dimensional time series are extended to determine the spatial frequencies at a specific point on a two dimensional surface or image. The two dimensional surface/image is sampled along a number of evenly angularly-spaced axes passing through the point of interest. The time-frequency analysis techniques are then applied to each of the one dimensional data sets. When taken together, the results form the Directional Spatial Frequency Distribution (DSFD), a two dimensional plot of spectral energy as a function of spatial frequency and the direction. When the two dimensional data consists of planar waves, a spatial correlation masking process can be used on the DSFD to produce a localized estimate of spatial frequency and direction of measurement called the Equivalent Planar Wave Sinusoidal Decomposition (EPWSD). The DSFD and EPWSD are calculated for simulated two dimensional data consisting of sinusoids and chirp signals from single and multiple directions as well as ocean wave measurements made by an airborne scanning radar altimeter and compared to a standard two dimensional Fourier transform. It is shown that the EPSWD technique provides a very localized estimate of frequency and direction of arrival even if the frequency is changing rapidly with position.

Keywords: time-frequency analysis, two dimensional frequency analysis, image analysis, ocean waves

2. INTRODUCTION

The time-frequency analysis techniques developed by Cohen and others[1,2, 3, 4] are able to accurately estimate the instantaneous frequency of a time series at a specific point in time even when the frequency of the signal is changing rapidly, unlike the spectrogram. The objective of this paper is to extend these techniques to estimate the *spatial frequencies present at a specific point* on a two dimensional surface/image.

The algorithm for analyzing the spatial frequency of two dimensional data is described in detail. This algorithm is then applied to simulated two dimensional data sets consisting of sinusoids and chirp signals from single and multiple directions of arrival. The results are compared to a standard two dimensional Fourier transform of the same data.

3. BACKGROUND

The most common method of time-frequency analysis is the spectrogram. A short segment of the entire data set is extracted and a Fourier transform is performed on this segment and its magnitude squared is the spectrogram. This process is repeated segment by segment until the entire data has been analyzed. The Fourier transforms of each of the segments are stacked together in time to form a time-frequency

0-8194-2234-7/96/$6.00

Downloaded From: http://proceedings.spiedigitallibrary.org/ on 11/08/2012 Terms of Use: http://spiedl.org/terms

distribution. Unfortunately, because of the time-bandwidth limitation, reducing the size of the time window to obtain better resolution in the time domain results in poorer resolution in the frequency domain.

Cohen introduced a general class of time-frequency distributions [1,2] which is described by the following equation where W is the Wigner distribution.

$$C_x(t,\omega) = \iint W_x(t-s,\omega-\nu)\psi(s,\nu)\,ds\,d\nu \qquad (1)$$

The properties of the resulting time-frequency distribution are directly affected by the kernel, ψ, that is used. The spectrogram is a member of Cohen's class. Using a different kernel than the one used by the spectrogram, we can reduce the effect of the time-bandwidth limitation due to windowing, resulting in improved resolution in both the time and frequency domains.

When signals made up of multiple components are analyzed, interference between Fourier transforms of the individual signal components produces artifacts in the time-frequency distribution. These artifacts are referred to as cross terms. A double exponential kernel was developed that suppresses the cross terms without excessively degrading the true signal components [3]. The so-called Alias-Free General Discrete-Time Time-Frequency Distribution (AFGDTFD), a discrete-time implementation of the Cohen's class that avoids aliasing problems encountered by earlier discrete-time implementations has also been developed [4]. The one dimensional time-frequency analyses performed as a part of this paper use the AFGDTFD implementation together with a Choi-Williams [3] exponential kernel.

4. METHOD

The algorithm for the Directional Spatial Frequency Distribution (DSFD) can be best explained for the case of a planar sinusoid which can then be generalized for other 2-dimensional signals. Consider a 2-dimensional data set of a single sinusoid given by the equation (2).

$$f(x,y) = A\cos\left(k\left(x\cos\theta + y\sin\theta\right)\right) \qquad (2)$$

Consider a planar sinusoid signal that has an amplitude, A =1; spatial frequency, k= 2π radians per unit distance and direction of arrival, θ =0 at the center point and throughout the two dimensional data set. This is shown in figure 1a.

Step 1: The two dimensional data set surrounding one specific point of interest is sampled along a number of evenly angularly spaced axes *passing through the point of interest.* In this example, the center point, (x,y) = (0,0) was selected as the point of interest. Bilinear interpolation is used to estimate the two dimensional surface/image at locations between the original x,y grid points. The number of axes is selected based on the angular resolution desired. In this example, 73 axes spaced at 5 degree increments (-180,-175...0...+175,+180 deg) are used.

The axial sampling effectively reduces the two dimensional data into 73 sets of one dimensional data, one for each sample axis. The result of this axial sampling process is shown in figures 1b and 1c. The figures 1b and 1c show the same axially sampled data, the only difference being that figure 1b is in the original x,y rectangular coordinate system while figure 1c shows the data in "rectipolar" format where the horizontal axis is the distance from the point of interest (labeled rho) and the vertical axis is the angle of the sample axis from the horizontal (labeled theta).

Downloaded From: http://proceedings.spiedigitallibrary.org/ on 11/08/2012 Terms of Use: http://spiedl.org/terms

Step 2: A separate time-frequency analysis is performed on each of the one dimensional axially sampled data sets using the Alias-Free General Discrete-Time Time-Frequency Distribution (AFGDTFD) technique developed by Jeong and Williams [3]. When this technique is normally used to analyze the frequency of a times series, the frequency is determined at all points in time, producing a time-frequency distribution. However, in this application, the spatial frequency of each axially sampled data set is only determined at *one point in space*, the point of interest. Therefore, only one spatial frequency spectrum is generated for each axially sampled data set. In our application, *the AFGDTFD time-frequency analysis technique is used to produce one, high resolution, estimate of the spatial frequency along each sample direction, applicable only at the point of interest where all of the sample axes intersect.* Using the AFGDTFD to estimate frequency instead of the Fourier transform means that the spatial frequency of two dimensional surfaces/images can be accurately determined even when the spatial frequency is changing rapidly with respect to space.

Step 3: The 73 separate spatial frequency estimates are then assembled into a single plot, shown in figure 1d. Each row of the plot consists of the spatial frequency estimate produced from each of the one dimensional axially sampled data sets. We have termed this the Directional Spatial Frequency Distribution (DSFD) or $D(k,\theta)$. The plot of $D(k,\theta)$ is in rectipolar format like figure 1c. The horizontal axis is the spatial frequency, k, and the vertical axis, θ, is the direction along which the one dimensional data were sampled.

From equation (2), the expected spatial frequency should be 2π radians per unit distance and the expected direction of arrival should be $\theta = 0$ degrees from the horizontal. This would be a single point on the DSFD. However, the DSFD in figure 1d shows a bow-shaped curve instead of a single point. At $\theta = 0$, the spatial frequency equals 2π as it should. However the DSFD seem to show that there is spectral power present at all other directions of arrival as well.

The explanation of this feature is related to the concept of "frequency of corrugation" [5]. The estimated spatial frequency has a maximum value and agrees with the expected value when the direction of measurement (the direction of the sampling axis) matches the direction of arrival ($\theta = 0$) of the two dimensional data set. As the direction of measurement gets farther away from the direction of arrival, the distance between successive wave peaks seen in the one dimensional axially sampled data set increases, resulting in an apparent reduction in the frequency. This is the concept of "frequency of corrugation". Even though the reason for the presence of the bow-shaped curve is clear, this could render the interpretation of the DSFD somewhat difficult. Therefore, we seek a method to transform the DSFD plot to one where in the above example, there will be a unique peak in the spatial frequency-direction of arrival plot at ($k = 2\pi, \theta = 0$).

Step 4: To the develop the required transformation, for a single planar sinusoidal wave, consider the relation between the true and measured frequency, which can be simply expressed as follows.

$$k = k_0\left(\cos(\theta - \theta_0)\right) \tag{3}$$

Here, k is the estimated frequency for the direction of measurement, θ; k_0 is the true spatial frequency (the expected answer); θ is the direction of measurement and θ_0 is the true direction of arrival of the wave front. It is easy to see that when plotted in the rectipolar format, the equation (3) describes the bow shaped curve in figure 1d. Therefore, when the presence of planar waves is suspected based on the DSFD or knowledge of the wave generation process, the following transformation is made to generate a plot which will have a unique peak in the spatial frequency-direction of arrival plane.

Downloaded From: http://proceedings.spiedigitallibrary.org/ on 11/08/2012 Terms of Use: http://spiedl.org/terms

Step 5: The DSFD is multiplied by a family of spatial masks based on equation (3). Each pair of (k_0,θ_0) define a bow-shaped spatial mask. The values of all DSFD points lying on this curve are summed together to obtain the result for that pair of (k_0,θ_0). This procedure is repeated for all (k_0,θ_0) pairs on the spatial frequency-direction of arrival plane. This technique is similar to the two dimensional spatial masking techniques commonly used in image processing[5].

Mathematically, the masking process can be described as follows. For a given (k_0,θ_0), a mask $M_0(k,\theta)$ is defined on the spatial frequency-direction of arrival plane as follows.

$$M_0(k,\theta) = 1 \quad when \quad k = k_0(\cos(\theta - \theta_0)) \\ = 0 \quad elsewhere \tag{4}$$

A point on the new surface, $P(k_0,\theta_0)$, is obtained as follows.

$$P(k_0,\theta) = \sum_k \sum_\theta D(k,\theta) M_0(k.\theta_0) \tag{5}$$

The result of applying this process to the DSFD in figure 1d is seen in 1e. The peak occurs at a spatial frequency of 2π and a direction of arrival of 0 degrees as expected. A second peak also occurs at a spatial frequency of 2π and direction of arrival of 180 degrees. This additional peak is the caused by the fact that a sinusoid is the sum of two complex exponentials with positive and negative frequencies. The transformed DSFD in figure 1e is called the "Equivalent Planar Wave Sinusoidal Decomposition (EPWSD)" denoted by $P(k_0,\theta_0)$ above, since it estimates how closely the two dimensional data set at the point of interest matches sinusoidal planar waves of varying spatial frequency and direction of arrival. While this mask is specific for planar waves, it can be modified to detect other types of wave fronts such as circular wave fronts by using different shaped masks.

The two dimensional Fourier transform (2DFT) of the two dimensional data set is shown in figure 1f. In figure 1f, spatial frequencies in the x and y directions are shown and the correct frequencies of 2 radians per unit distance along the x-direction and 0 radians per unit distance along the y-direction has been estimated. The direction of arrival at the center point is the angle the peak makes with the center point and can be seen to be equal to 0 degrees.

To clarify the information provided by DSFD, EPWSD and 2DFT, an additional example of 3 planar sinusoids is considered. The two dimensional data set consists of the sum of three planar sinusoids, similar to equation (2), with the following spatial frequencies and directions of arrival at the center point (and throughout the two dimensional data set): $(k_0,\theta_0) = (2\pi, 0)$; $(6\pi, 25)$ and $(4\pi, 75)$.

The figure 2a shows the two dimensional surface. It is difficult to identify what frequencies and directions of arrival are present. The figure 2b is the DSFD for this signal. Three sets of bows can be seen. The figure 2c is the EPWSD of this signal. The peaks are located at the correct spatial frequencies and directions of arrival. The figure 2d is the 2DFT of the signal. It shows the three peaks at the proper spatial frequency locations and directions of arrival (angles each of the peaks subtend at the center point).

The analysis of single and multiple planar waves show that the EPWSD and 2DFT provide consistent information for simple two dimensional data sets. However, when spatial frequencies are not constant (such as chirps), the EPWSD is superior to 2DFT as demonstrated below.

Downloaded From: http://proceedings.spiedigitallibrary.org/ on 11/08/2012 Terms of Use: http://spiedl.org/terms

5. RESULTS & DISCUSSION

The results from performing the analysis described in the previous section on examples where spatial frequencies are not constant are discussed below. The method is then applied to ocean wave height data to demonstrate its ability to estimate spatial frequencies and directions of arrival at a selected location.

Case(1) 1 Planar Chirp: The two dimensional data set used in this example consists a single chirp sweep in frequency as the position changes. The equation of the two dimensional chirp signal is as follows.

$$f(x,y) = \left(\frac{0.01}{\pi}\right)^{1/4} e^{(0.05r)+j(r+10r)};\ \textit{where}\ r = x\cos(\theta_0) + y\cos(\theta_0) \qquad (6)$$

The spatial frequency at any point, (x,y), is $k_o = \frac{d}{dr}(r^2 + 10r)$. The spatial frequency at the center point is k_0 = 2r+10 = 10 and direction of arrival at the center point is chosen to be 0 degrees, i.e., at the *center point only*, $(k_0,\theta_0)=(10,0)$. In figure 3a, the two dimensional surface is shown. The DSFD and the EPWSD of this signal is shown in figures 3b and 3c. The peak on the EPWSD is located at the correct spatial frequency and direction of arrival. The 2DFT for the signal is shown in figure 3d. It shows the correct direction of arrival, but the frequency estimate is smeared over a range of frequencies.

Case(2) 3 Planar Chirps: The two dimensional data set used in this example consists a three chirps sweeping in frequency as the position changes. The spatial frequencies and directions of arrival of the signal at the *center point only* are (k_0,θ_0) = (10, 0); (10, 25) and (10, 75). In figure 4a, the two dimensional surface is shown. The figure 4b is the DSFD and figure 4c is the EPWSD of this signal. The peaks on the EPWSD are located at the correct spatial frequencies and directions of arrival. The 2DFT for the signal is shown in figure 4d. It shows the correct directions of arrival, but the frequency estimate is smeared over a range of frequencies.

The analysis of single and multiple planar chirps demonstrate that the EPWSD method can correctly estimate the spatial frequencies and directions of the planar waves where as the 2DFT method cannot when the spatial frequencies are variable.

Case(3) Ocean Wave Data : The two dimensional data set consists of ocean wave height measurements made by NASA and the U.S. Navy using a scanning radar altimeter installed onboard a P-3 aircraft[6]. This data set was collected off the coast of North Carolina as a part of the DUCK94 field test. The data set was collected in a 64 x 64 grid that covering a 550 meter by 428 meter area of the ocean. This data set was interpolated at 2.5 m intervals before it was analyzed. A 400 meter diameter area in the center of the data set was used in the following analysis. Case 3A and Case 3B used the same data set except that the center point of the analysis was shifted by 100 meters.

Case(3A): In figures 5a and 5b, the surface and contour plots are shown. In figure 5b, four parallel wave fronts can be seen, travelling from left to right and slightly upwards. These wave fronts are marked with solid lines and labeled A, B, C and D. In addition, a single partial wave front, labeled E, is located near the center of the plot travelling upwards and slightly to the left. The center point for the analysis is located in a trough between wave front B and C and is marked by a '+' in figure 5b.

In figure 5c, the EPSWD of the ocean wave data is shown. There is a single peak present, with a direction of arrival of 25 degrees and a radial spatial frequency of 0.05 radians per meter (125 meter wavelength). The 2DFT of the ocean wave data is shown in figure 5d. There is a single peak with a direction of arrival of 20 degrees and a spatial frequency of 0.05 radians per meter (125 meter wavelength).

Downloaded From: http://proceedings.spiedigitallibrary.org/ on 11/08/2012 Terms of Use: http://spiedl.org/terms

There is close agreement between the EPSWD and the 2DFT. The direction of arrival estimates produced by the EPSWD and 2D FFT are shown on Figure 33 as dashed lines labeled 'EPSWD' and '2D FFT', respectively . The direction of arrival estimates produced by the EPSWD and 2DFT agree well with the normal to wave fronts A, B, C and D. In addition, the spatial frequency / wavelength estimates produced by the EPSWD and 2DFT also agree well with the spacing between wave fronts A, B, C and D.

Case(3B): In figures 6a and 6b, the surface and contour plots of the ocean surface are shown. In figure 6b, the same wave fronts present in Case 3B are still present and have been marked and labeled as before. The only difference from Case 3A is that the center point of the analysis is now located where wave front C and E intersect. The center point is marked by a '+' in figure 6b.

In figure 6c, the DSFD of the ocean wave data is shown. Peaks are present with directions of arrival of 115, 95 and 30 degrees. The peaks at 115 degrees have spatial frequencies of 0.01 radians per meter (628 meter wavelength) and 0.06 radians per meter (105 meter wavelength). The peak at 95 degrees has a spatial frequency of 0.01 radians per meter (628 meter wavelength). The peaks at 30 degrees have spatial frequencies of 0.01 radians per meter (628 meter wavelength) and 0.09 radians per meter (70 meter wavelength). No bow shaped curves are apparent in the DSFD. Because the DSFD already has peaks and shows no bow shaped curves, applying the spatial correlation filter to produce the EPSWD does not provide additional information.

The direction of arrival estimates produced by the DSFD are shown on figure 6c as 3 dashed lines labeled 'DSFD'. These estimated directions of arrival match reasonably well with the upper and lower sections of wave front C and wave front E, all of which pass through the center point. Note that wave front C is not straight and bends near the center point.

Figure 6d shows the 2DFT for the signal. This figure shows a peak with a direction of arrival of about 20 degrees and a radial spatial frequency of 0.05 radians per meter (125 meter wavelength) This result is the same as for Case 3B. This similarity is caused by the large overlap of the ocean wave data used in Case 3A and Case 3B.

Figure 6e is the ocean wave height profile along the 115 degree axis. The line labeled '105 m' shows the peaks spaced at the wavelength estimated by the DSFD. The low frequency component (0.01 radians per meter/ 628 meter) is apparent in this profile and is caused by the 115 degree sample axis first passing along the lower section of wave front C and then along the trough between the upper sections of wave front B and C.

Figure 6f is the ocean wave height profile along the 95 degree axis. The low frequency component (0.01 radians per meter/ 628 meter) is apparent in this profile and is caused by the 95 degree sample axis first passing along the trough between the lower sections of wave front B and C. and then along the upper section of wave front C.

Figure 6g is the ocean wave height profile along the 30 degree axis. The line labeled '70 m' shows the peaks spaced at the wavelength estimated by the DSFD. The low frequency component (0.01 radians per meter/ 628 meter) is apparent in this profile and is caused by the 30 degree sample axis first passing along wave front E and then along the trough between wave front C and D.

Summary: Case 3A and Case 3B show that the DSFD and EPSWD change radically when the center point is moved on the same surface. This expected because the wave patterns in the vicinity of the two center points were radically different. These cases also show that the results from the DSFD and EPSWD can be related to features on the surface near the center point.

Downloaded From: http://proceedings.spiedigitallibrary.org/ on 11/08/2012 Terms of Use: http://spiedl.org/terms

In Case 3A, the EPSWD agreed with the 2DFT. This probably occurred because the center point was located near, but not on top of , two of the parallel wave fronts B and C. On the other hand, in Case 3B the DSFD had peaks while the EPSWD did not. This probably occurred because the center point was located on top of the crest of three wave fronts. As a result, the wave fronts only appeared in a small number of sample axes. This prevented the spatial correlation filter that produces the EPSWD from finding the wave front. Because of the large spectral energy along the crests, the DSFD was able to detect these wave fronts.

It appears that the characteristics of the 2DFT, DSFD and EPSWD complement each other. The 2DFT performs well against a repetitive pattern that does not change across a surface. The DSFD detects wave fronts oriented radially from the center point. And the EPSWD detects wave fronts wave fronts oriented tangentially to the center point.

6. CONCLUSIONS

A new approach to extending time-frequency analysis techniques to handle 2-dimensional data has been successfully demonstrated. It provides the capability to determine the frequency content at a specific point on a two dimensional surface or image whose frequency is changing rapidly.

Currently, the DSFD and EPWSD are being applied to more examples of ocean wave measurements made by an airborne scanning radar altimeter. One possible application of the results might be to attempt the indirect measurement of water depth near shore by analyzing the scanning radar altimeter DSFD-EPWSD to detect shifts in the frequency and direction of oceans wave that occurs as the waves approach shore. Another area of application might be the analysis of texture of images at specific points of interest or the vibration patterns of structures. The DSFD-EPWSD method is being extended in its practical applicability with the incorporation of the Kalman time-frequency distribution. Such an optimal filter formulation allows for the estimation of TFDs of random or noisy signals[7]. The Kalman-TFD based DSFD and EPWSD is expected to provide very localized estimate of frequency and direction of arrival from noisy measurements even if the frequency is changing rapidly with position.

7. ACKNOWLEDGEMENTS

One of the authors (DEH) would like to thank Dr. Marshall Earle of Neptune Sciences, Inc., Dr Edward Walsh of NASA and Dr. Janice Boyd of the Naval Research Laboratory for allowing us to use the scanning radar altimeter wave height data from the DUCK94 exercise[6].

8. REFERENCES

1. L. Cohen, "Generalized phase-space distribution functions," Math. Phys., vol. 7, pp. 781-786, 1966.
2. L. Cohen, "Time-Frequency Analysis," Prentice-Hall, 1994.
3. H. Choi and W. Williams, "Improved time-frequency representation of multicomponent signals using exponential kernels," IEEE Trans. on ASSP, vol 37, pp. 862-871, June 1989.
4. J. Jeong and W. Williams, "Alias-free generalized discrete-time time-frequency distributions," IEEE Trans. on Signal Processing, vol 40, pp. 2757-2765, November 1992.
5. R.N. Bracewell, "Two-Dimensional Imaging", Prentice-Hall, 1995.
6. M. Earle, E. Walsh, J. Boyd, "Scanning Radar Altimeter Sea Surface Topography and High-Resolution Directional Wave Measurements,"The DUCK94 Nearshore Field Experiment Report, June 1994
7. P.G. Madhavan and W.J. Williams, "A Time Varying Model for the Estimation of Time Frequency Distribution of Signals in the Presence of Noise", IEEE Signal Processing Letters, 1996 (submitted).

Downloaded From: http://proceedings.spiedigitallibrary.org/ on 11/08/2012 Terms of Use: http://spiedl.org/terms

Fig 1a - Surface - 1 Planar Sinusoid

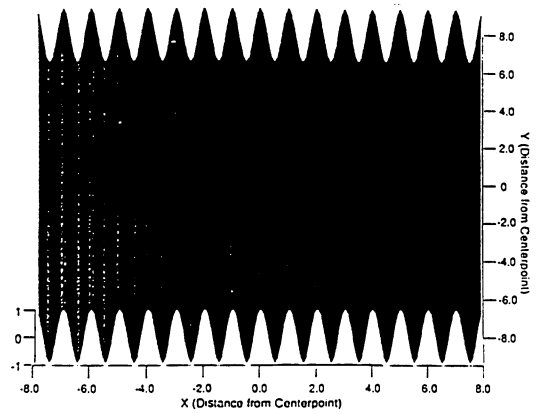

Fig 1b - Surface - Sampled (Rect)

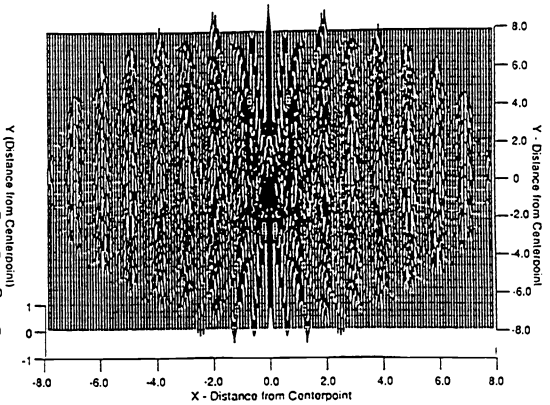

Fig 1c - Surface - Sampled (Polar)

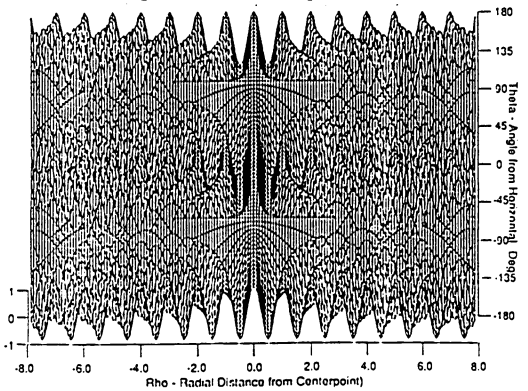

Fig 1d - DSFD

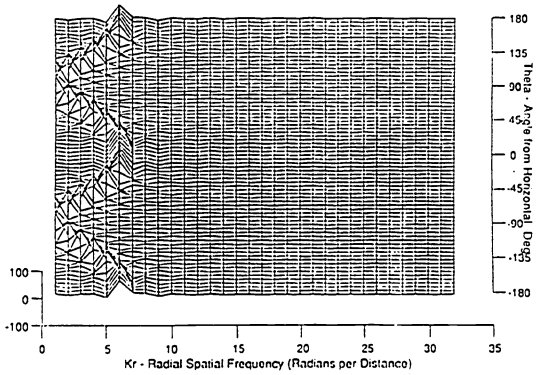

Fig 1e - EPSWD

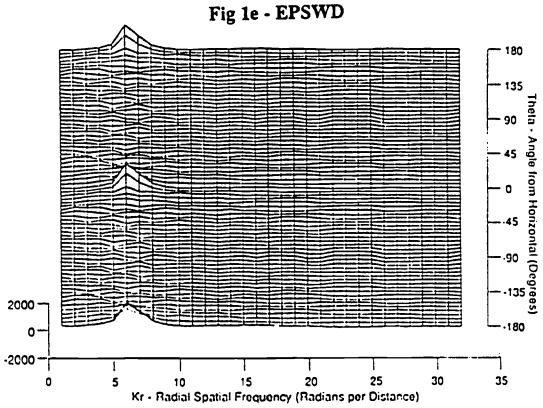

Fig 1f - 2D FFT

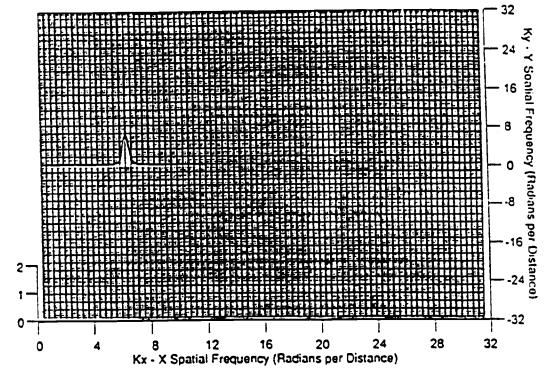

Downloaded From: http://proceedings.spiedigitallibrary.org/ on 11/08/2012 Terms of Use: http://spiedl.org/terms

Fig 2a - Surface - 3 Planar Sinusoids

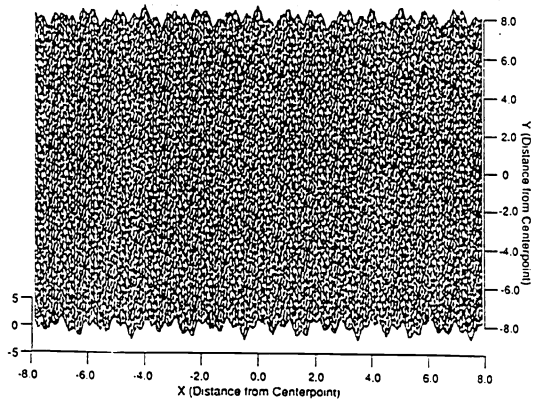

Fig 2b - DSFD

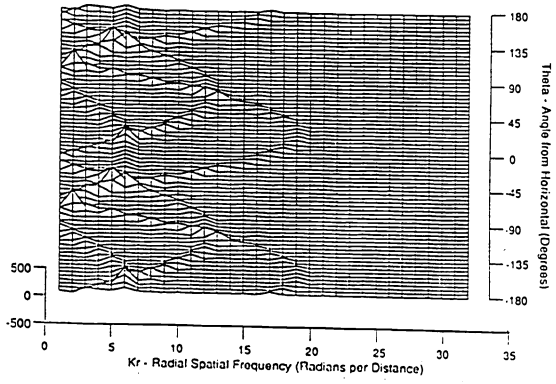

Fig 2c - EPSWD

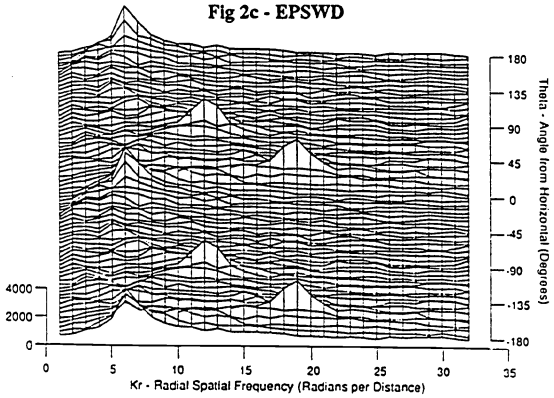

Fig 2d - 2D FFT

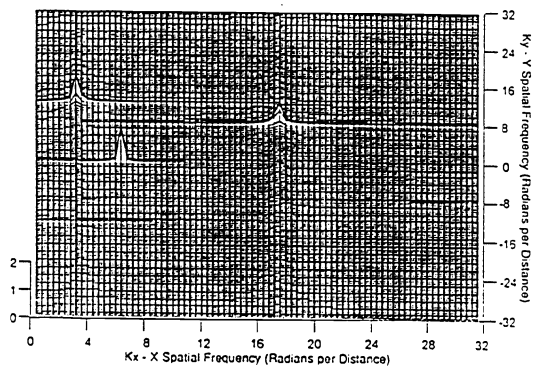

Fig 3a - Surface - 1 Planar Chirp

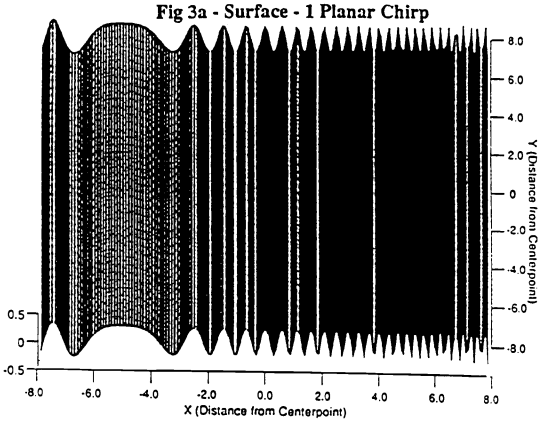

Fig 3b - DSFD

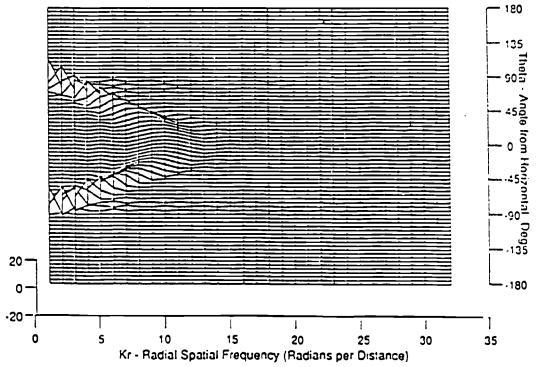

Fig 3c - EPSWD

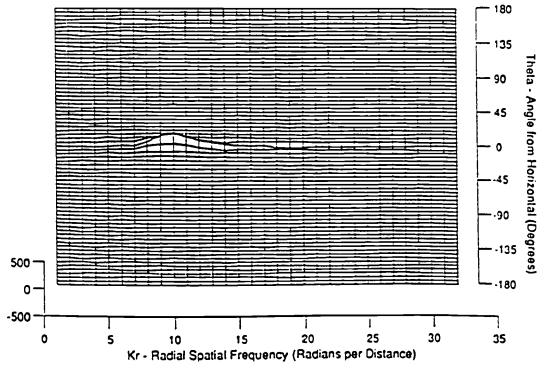

Fig 3d - 2D FFT

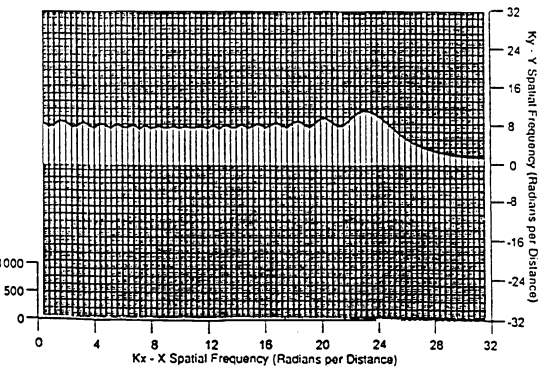

Downloaded From: http://proceedings.spiedigitallibrary.org/ on 11/08/2012 Terms of Use: http://spiedl.org/terms

Fig 4a - Surface - 3 Planar Chirps

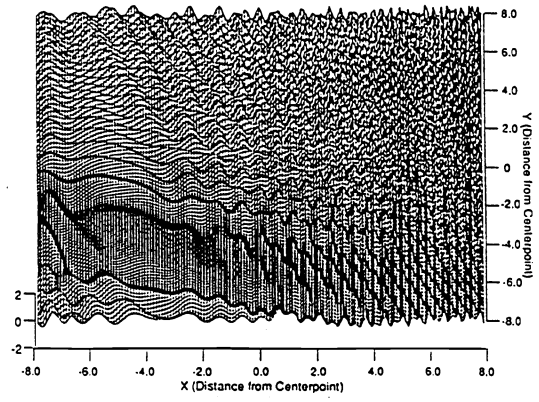

Fig 4b - DSFD

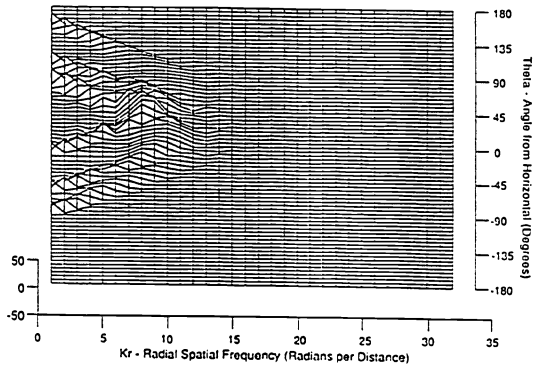

Fig 4c - EPSWD

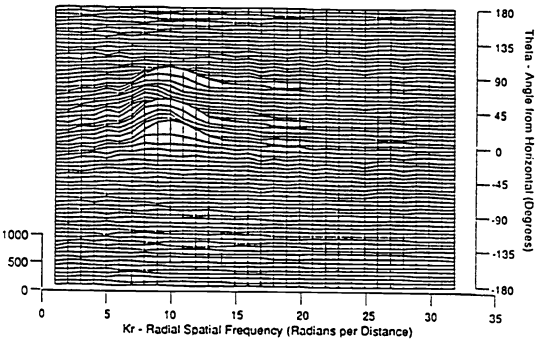

Fig 4d - 2D FFT

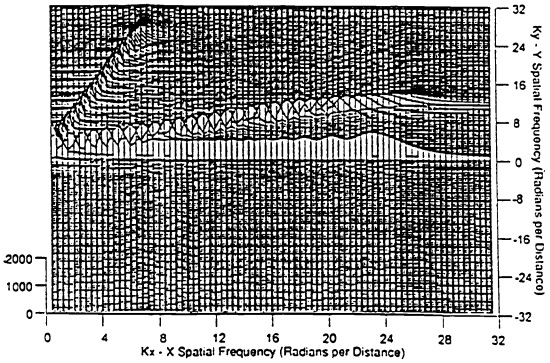

Fig 5a - Surface - Ocean Wave Data - Case 3A

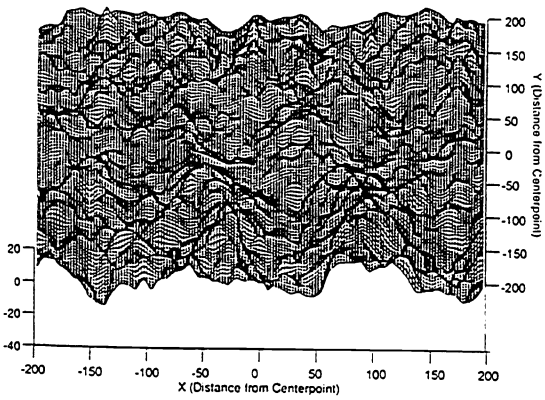

Fig 5b - Surface - Ocean Wave Data (Contour)

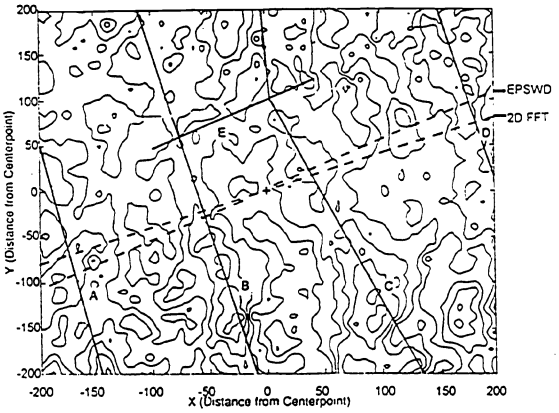

Fig 5c - EPSWD

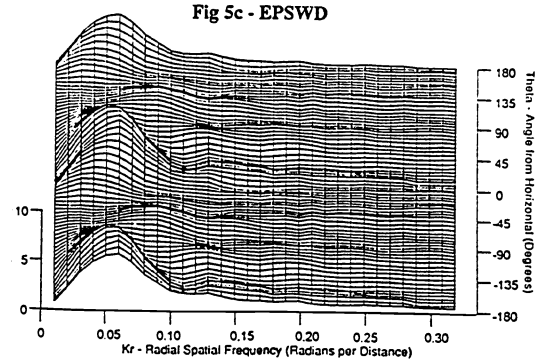

Fig 5d - 2D FFT

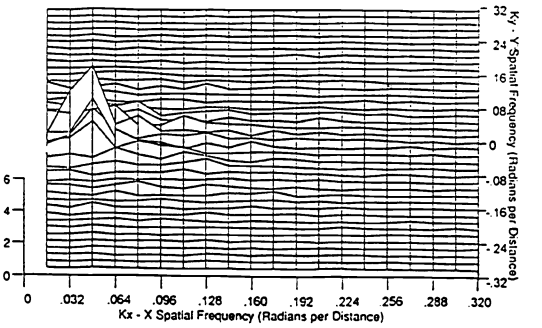

Downloaded From: http://proceedings.spiedigitallibrary.org/ on 11/08/2012 Terms of Use: http://spiedl.org/terms

Fig 6a - Surface - Ocean Wave Data - Case 3B

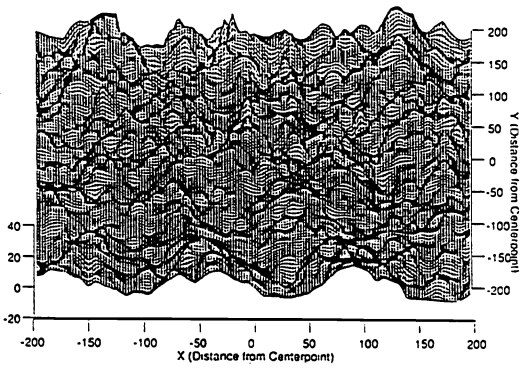

Fig 6b - Surface - Ocean Wave Data (Contour)

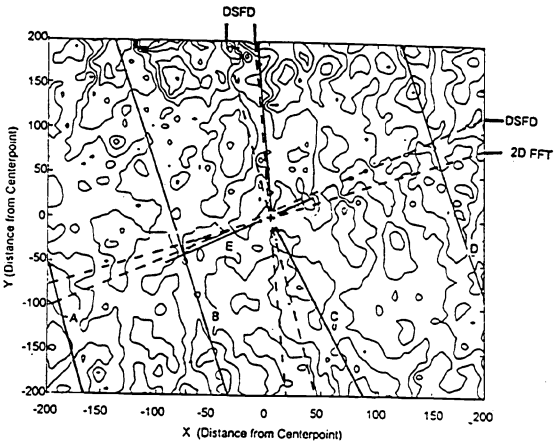

Fig 6c - DSFD

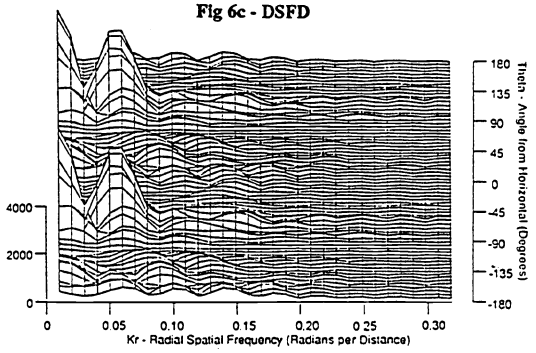

Fig 6d - 2D FFT

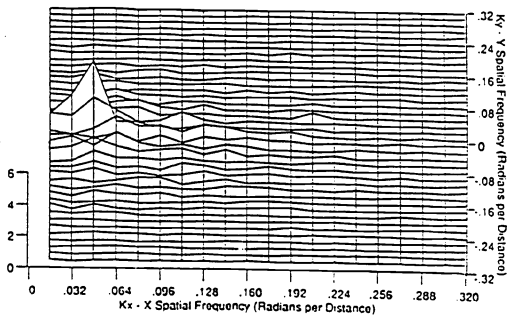

Fig 6e - Wave Height Along 115 deg

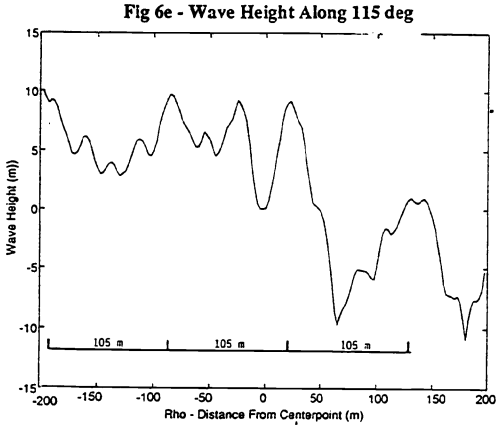

Fig 6f - Wave Height Along 95 deg

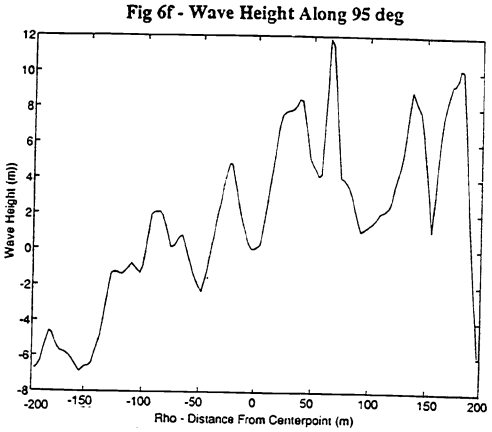

Fig 6g - Wave Height Along 30 deg

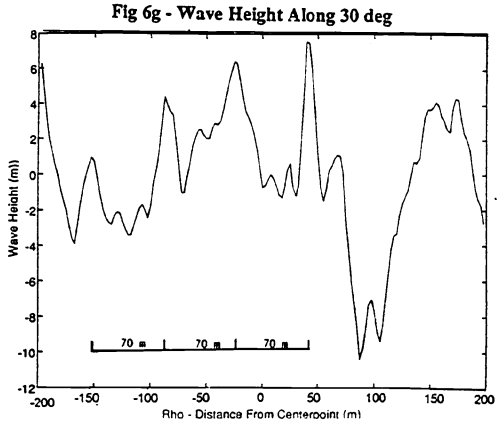

Downloaded From: http://proceedings.spiedigitallibrary.org/ on 11/08/2012 Terms of Use: http://spiedl.org/terms